

Central Lancashire Online Knowledge (CLOK)

Title	Accraspiroketides A-B, Phenyl-naphthacenoid-Derived Polyketides with Unprecedented [6 + 6+6 + 6] + [5 + 5] Spiro-Architecture
Type	Article
URL	https://clock.uclan.ac.uk/51080/
DOI	https://doi.org/10.1021/acs.jnatprod.3c01012
Date	2024
Citation	Maglangit, Fleurdeliz, Wang, Shan, Moser, Arvin, Kyeremeh, Kwaku, Trembleau, Laurent, Zhou, Yongjun, Clark, David James, Tabudravu, Jioji and Deng, Hai (2024) Accraspiroketides A-B, Phenyl-naphthacenoid-Derived Polyketides with Unprecedented [6 + 6+6 + 6] + [5 + 5] Spiro-Architecture. <i>Journal of Natural Products</i> , 87 (4). pp. 831-836. ISSN 0163-3864
Creators	Maglangit, Fleurdeliz, Wang, Shan, Moser, Arvin, Kyeremeh, Kwaku, Trembleau, Laurent, Zhou, Yongjun, Clark, David James, Tabudravu, Jioji and Deng, Hai

It is advisable to refer to the publisher's version if you intend to cite from the work.
<https://doi.org/10.1021/acs.jnatprod.3c01012>

For information about Research at UCLan please go to <http://www.uclan.ac.uk/research/>

All outputs in CLOK are protected by Intellectual Property Rights law, including Copyright law. Copyright, IPR and Moral Rights for the works on this site are retained by the individual authors and/or other copyright owners. Terms and conditions for use of this material are defined in the <http://clock.uclan.ac.uk/policies/>

Accraspiroketides A-B, phenylnaphthacenoid-
derived polyketides with unprecedented [6+6+6+6]
+ [5+5] spiro-architecture

*Fleurdeliz Maglangit**, *Shan Wang*, *Arvin Moser**, *Kwaku Kyeremeh*, *Laurent Trembleau*,
Yongjun Zhou, *David James Clark*, *Jioji Tabudravu**, *Hai Deng**

Fleurdeliz Maglangit - Department of Biology and Environmental Science, College of Science,
University of the Philippines Cebu, Gorordo Ave., Lahug, Cebu City, Philippines

Shan Wang - State Key Laboratory of Microbial Technology, Shandong University, Qingdao
266237, China

Kwaku Kyeremeh - Department of Chemistry, University of Ghana, P.O. Box LG56 Legon-
Accra, Ghana

Laurent Trembleau - Department of Chemistry, University of Aberdeen, Meston Walk,
Aberdeen AB24 3UE, Scotland, UK

Yongjun Zhou - Research Center for Marine Drugs, State Key Laboratory of Oncogenes and
Related Genes, Department of Pharmacy, Ren Ji Hospital, School of Medicine, Shanghai Jiao
Tong University, Shanghai 200127, China

David James Clark - EastChem, School of Chemistry, University of Edinburgh, Edinburgh
EH9 3FJ, UK

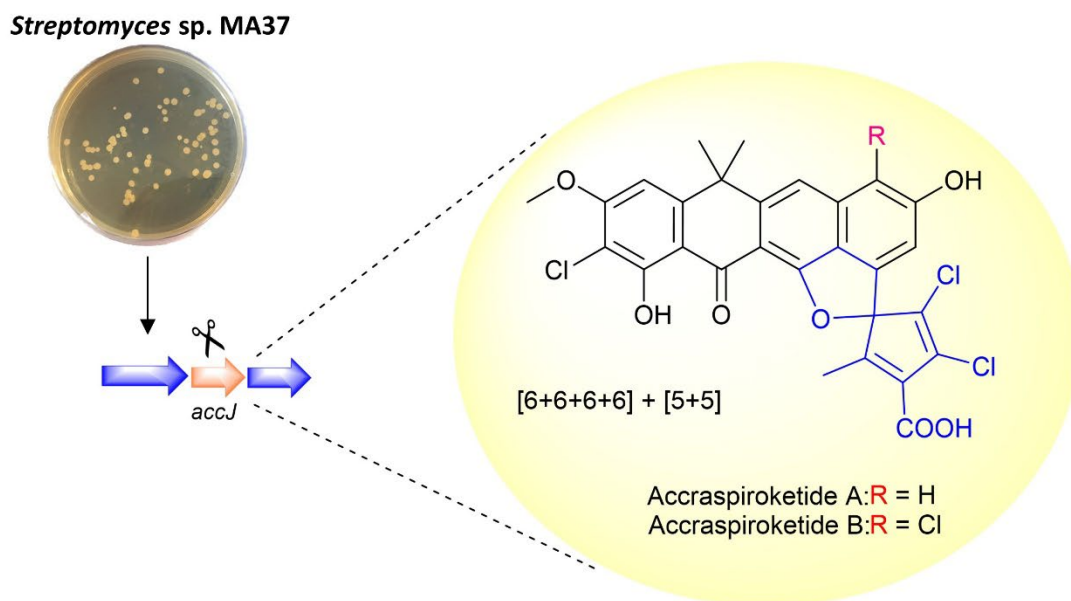
Arvin Moser - ACD/Labs, Advanced Chemistry Development, Toronto Department, 8 King
Street East, Suite 107, Toronto, Ontario, M5C 1B5, Canada

Bruce F. Milne - CFisUC, Department of Physics, University of Coimbra, Rua Larga, 3004-516
Coimbra, Portugal

Jioji Tabudravu - School of Pharmacy and Biomedical Sciences, University of Central
Lancashire, PR1 2HE, Preston, UK

Hai Deng - Department of Chemistry, University of Aberdeen, Meston Walk, Aberdeen AB24
3UE, Scotland, UK

Two novel polyketides, accraspiroketides A (**1**) and B (**2**), which feature an unprecedented [6+6+6+6] + [5+5] spiro chemical architectures, were isolated from *Streptomyces* sp. MA37 $\Delta accJ$ mutant strain. Compounds **1-2** exhibit excellent activity against Gram-positive bacteria (MIC = 1.5–6.3 $\mu\text{g/mL}$). Notably, **1** and **2** have superior activity against *Enterococcus faecium* K60-39 clinical isolate (MIC = 4.0 $\mu\text{g/mL}$ and 4.7 $\mu\text{g/mL}$, respectively) than ampicillin antibiotic (MIC = 25 $\mu\text{g/mL}$).



Phenyl-naphthacenoid polyketides (PNPs) have received significant attention recently owing to their potent antibacterial and cytotoxic activities.¹ To date, over 100 members of PNPs have been reported from various *Streptomyces* species under the names accramycins,^{2,3} fasamycins,⁴ naphthacemycins,⁵ formicamycins,⁶ formicapiridines,⁷ streptovertimycins,⁸ and streptovertidiones⁹ (Figure S1).

Accramycins are produced from the talented soil bacterium *Streptomyces* sp. MA37.^{2,3,10-14} They display potent antimicrobial activities against clinically relevant Gram-positive pathogens, including Enterococci clinical isolates.^{2,3} Their production in MA37 is controlled by the MarR-family regulator *accJ* in the accramycin (*acc*) biosynthetic gene cluster (BGC).² Deletion of *accJ* increased products of the *acc* pathway by up to 330-fold in the host producer. We have also identified other polyketides from $\Delta accJ$ strain isolated from bacteria for the first time.¹³ Consistent with these findings, the deletion of *forJ*, a homolog of *accJ* in *Streptomyces formicae* KY5, also increased the total productivity of formicamycin and fasamycin metabolites by six-fold.¹⁵

Continued mining of bioactive metabolites from the $\Delta accJ$ mutant strain revealed peaks with distinct UV patterns (λ_{max} 225, 245, 285, 305, 335, 350, 390 nm) (Figure S25) unique from the characteristic UV spectrum of the accramycin chromophore (Figure S26).^{2,3} Repeated chromatography of the $\Delta accJ$ extracts led to the isolation of two novel polyketides, accraspiroketides A (**1**) and B (**2**), with an unprecedented spiro ring system (Figure 1).

RESULTS AND DISCUSSION

The isolated yellow solid **1** was named accraspiroketide A after Accra, Ghana, where the soil samples were taken.^{10,12} From high-resolution mass spectrometry (HRESIMS) measurements (m/z 573.0270) in the positive mode (Figures S2), we deduced that accraspiroketide A (**1**) has a

molecular formula of $C_{28}H_{19}Cl_3O_7$ with eighteen indices of hydrogen deficiency (Figure 1, Table 1). The 1H NMR spectrum of **1** in CD_3CN (Figure S3) displayed signals arising from one methoxy group (δ_H 4.06), three methyl groups (δ_H 1.84, 1.85, 1.67), four methines (δ_H 7.52, 7.03, 6.93, 6.69), and one exchangeable hydroxy proton (δ_H 14.86), suggesting the presence of two more exchangeable protons in the structure of **1** (Table 1). The ^{13}C NMR data generated from the 1H - ^{13}C HSQC and HMBC spectra (Figures S4-S6) is indicative of a polycyclic aromatic system with 28 carbons corresponding to the above protonated units ($4 \times CH_3$, $4 \times CH$) and 20 non-protonated carbons including one carbonyl (δ_C 186.3), one carboxylic acid (δ_C 169.5), three chloro-substituted carbons (δ_C 109.9, 133.1, 133.4), and one sp^3 oxygenated carbon (δ_C 96.9). Overall, the spectroscopic data revealed that accraspiroketide A (**1**) contained the [6+6+6+6] (or dimethyltetracen-5-(12*H*)-one core) (rings A-D) similar to the accramycins reported previously.^{2,3} Major structural differences of **1** from accramycin compounds were identified, including striking low- to high-field or high- to low-field chemical shifts for three carbons, C-8 (δ_C 161.5), and C-9 (δ_C 123.2), and C-10 (δ_C 146.3), as well as the appearance of new signals corresponding to dichloro-substituted spirocycles with a carboxylic acid motif. The presence of the carboxylic acid moiety was further confirmed by the MS² fragmentation in the negative HRMS mode, as evidenced by 44 Da loss (Figures S14, S17-18)

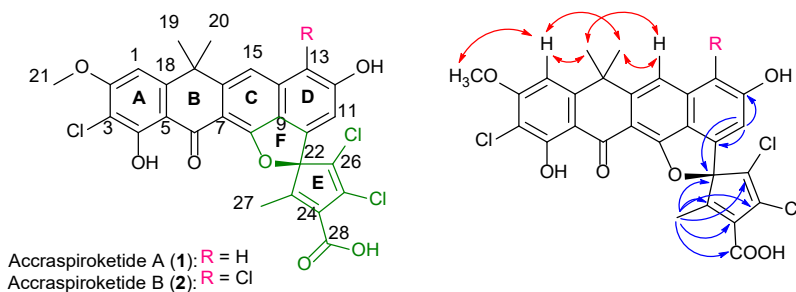


Figure 1. Accraspiroketides A (**1**) and B (**2**) with NOESY (\leftrightarrow) and key HMBC (\rightarrow) correlations

Rings A-D plus one ketone, plus one carboxylic acid, plus 20 sp^2 carbons accounted for 16 of the 18 indices of hydrogen deficiencies, suggesting the presence of two additional rings (E and F) in the structure of **1**. One of the rings was deduced from HMBC correlations of H-27 (δ_H 1.67) with C-22 (δ_C 96.9), C-23 (δ_C 136.8), C-24 (δ_C 132.6), C-25 (δ_C 133.1), C-26 (δ_C 133.4), and C-28 (δ_C 169.5) establishing the presence of the *dichloro*-substituted carbocycle with a carboxylic acid scaffold (ring E) (Figure 1, Table 1). HMBC correlations from H-11 (δ_C 6.69) to C-22 (δ_C 96.9) established connections between rings D and E. However, the assignments of the remaining oxygen in the formula and the positions of carboxylic acid, methyl, dichloro-substituents in either 5- or 6-membered rings in the remaining parts of the structure presented a challenge. Two possible structures were proposed, both of which contain a carboxylic acid (Figure S15). The first possibility could be a pyran ring fused with the pentacyclic Ring E where the methyl group is placed at the bridge of the pyran and Ring E. The other could be a spiro-furan structure where the methyl group is placed in the pentacyclic ring. To determine which of the two possible structures is correct and help assign the correct substitution patterns, computer-assisted structure elucidation (CASE) was performed.¹⁶ The ACD/Structure Elucidator has been used to successfully elucidate and verify structures of complex natural products, resolve structural ambiguities,¹⁷⁻²¹ and predict correct structures calculated by DFT.²¹ To this end, we entered the 1D and 2D NMR and the molecular formula based on the MS spectral data of **1** and the mandatory -COOH, (and -COO⁻) fragments into ACD/Structure Elucidator, and performed calculations using correlation spectroscopy-based generator (CSB) using both standard and ‘fuzzy’ generation mode (Figure S16). For the -COOH fragment, a total of 1,304 unique candidate structures were generated (Figure S16a) where the proposed spiro-furan structure was ranked 1 while the structure with the pyran ring was ranked 13 (Figure 1, Figure S16a). Ranking is based on overall chemical shift

deviations between experimental and predicted values using the HOSE code (dA = 2.9 ppm; Figures S16a) which is within the errors known to produce correct structures calculated by the ACD/Labs Structure Elucidator.^{16,19} Similar results were obtained using the -COO⁻ fragment (Figure S16b) where the spiro-furan structure was ranked 1 (dA = 3.0) while the pyran ring containing structure was ranked 10 out of 2,776 possible structural isomers. Further calculations were performed using NMR data acquired in DMSO-*d*₆ (Figures S20-22), the result (Figure S23) showed the proposed structure (Figure 1) was the only structural candidate. A plot of ¹³C predicted chemical shifts (calculated by ACD/Structure Elucidator) against experimental chemical shifts in CD₃CN showed an excellent linear correlation with $R^2 = 0.999$ (Figure S19a-b) (Figure S24 for DMSO-*d*₆), further supporting the proposed structure for **1** (Figure 1). Further evidence for **1** is provided by the fragmentation patterns in MS² analysis (Figures S14, S17-18). Taken together, the structure of **1** was deduced to feature an unprecedented chemical architecture consisting of [6+6+6+6] fused to a [5+5] spiro-ring system. The absolute configuration of C-23 in **1** was determined to be *R* configuration. This assignment was supported by a comparison between the time-dependent density functional theory (TDDFT) and experimental electronic circular dichroism (ECD) spectra of **1** (Figure 2, Table S3).

Table 1. ¹H (800 MHz) and ¹³C-NMR (200 MHz) data of accraspiroketide A (**1**) in CD₃CN.

No.	¹³ C ppm	¹ H ppm, mult. (<i>J</i> , Hz)	COSY	NOESY	HMBC
1	101.2, CH	6.93, s	-	19, 20, 21	21, 17, 5, 3, 18, 6
2	160.2, C	-	-	-	1, 21
3	109.9, C	-	-	-	1, 31
4	159.8, C	-	-	-	OH
5	106.0, C	-	-	-	1, 31
6	186.3, C	-	-	-	1, 15
7	106.3, C	-	-	-	15

No.	¹³ C ppm	¹ H ppm, mult. (J, Hz)	COSY	NOESY	HMBC
8	161.5, C	-	-	-	11, 13
9	123.2, C	-	-	-	11, 13, 15
10	146.3, C	-	-	-	11, 15
11	107.3, CH	6.69, d (1.5)	13	-	8, 9, 10, 13, 22
12	165.3, C	-	-	-	13, 15
13	106.2, CH	7.03, d (1.5)	11	15	8, 9, 11, 12, 15
14	134.9, C	-	-	-	15
15	112.5, CH	7.52, s	-	13, 19, 20	6, 7, 9, 10, 12, 13, 14, 17
16	150.1, C	-	-	-	19, 20
17	39.8, C	-	-	-	1, 15, 19
18	151.8, C	-	-	-	1, 19, 20
19	33.5, CH ₃	1.84, s	-	1, 15	16, 17, 18, 20
20	34.0, CH ₃	1.85, s	-	1, 15	16, 18, 19
21	56.2, CH ₃	4.06, s	-	1	1
22	96.9, C	-	-	-	11, 27
23	136.8, C	-	-	-	27
24	132.6*, C	-	-	-	27
25	133.1*, C	-	-	-	27
26	133.4*, C	-	-	-	27
27	14.4, CH ₃	1.67, s	-	-	22, 23, 24, 25, 26, 28
28	169.5, C	-	-	-	27
	-	14.86, s, OH	-	-	3, 4, 5

* ¹³C chemical shifts overlapped in ¹H-¹³C HMBC and correlated with predicted ¹³C chemical shifts.

Accraspiroketide B (**2**) was obtained as a yellow solid. The structure of **2** was tentatively deduced based on HRESIMS (Figure S9) analysis and partial NMR data (Figure S10-S13, Table S1). The molecular formula of C₂₈H₁₈Cl₄O₇ and MS isotopic pattern (Figure S9) indicated the presence of 4 chlorines in the structure of **2**.²² The position of the extra chlorine in **2** was established by analysis of NMR data where H-11 was now showing as a singlet rather than a

doublet as in **1** suggesting that the extra chlorine group was occupying position C-13 instead of a proton as in **1**. In addition, HMBC correlations from H-11 (δ_{H} 6.82) to C-9 (δ_{C} 123.2) and C-13 (δ_{C} 112.0). This was also supported by a comparison of the chemical shifts of chlorine-substituted compounds at C-13 (*i.e.*, accramycins F and J), previously isolated from MA37.² Compound **2** has eighteen indices of hydrogen deficiency, similar to **1**. Other spectroscopic features of **2** were similar to those of **1**, except for the additional chlorine moiety and some carbon signals (C4, C6, C8, C26, and C28) that were not detected in 600 MHz NMR due to the minute amount of the sample. Nevertheless, the spiro ring system was deduced from HMBC correlations from H-27 (δ_{H} 1.75) to C-22 (δ_{C} 96.0), C-23 (δ_{C} 138.7) and C-24 (δ_{C} 131.2) (Figure S12, Table S1). The UV profiles of compounds **1** and **2** are identical (Figure S25), indicating that they are of identical chromophores and chemical backbone. This UV profile is distinct from those of accramycins isolated from MA37 previously (Figure S26).^{2,3,13}

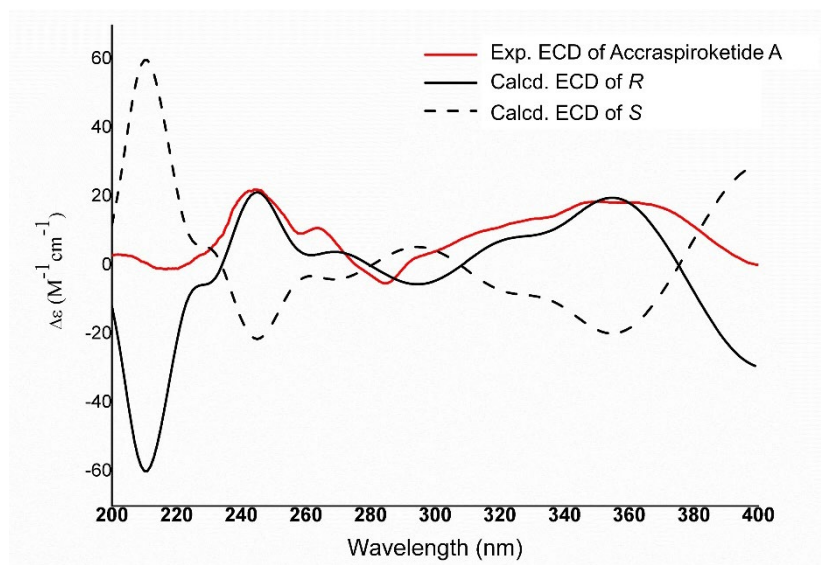


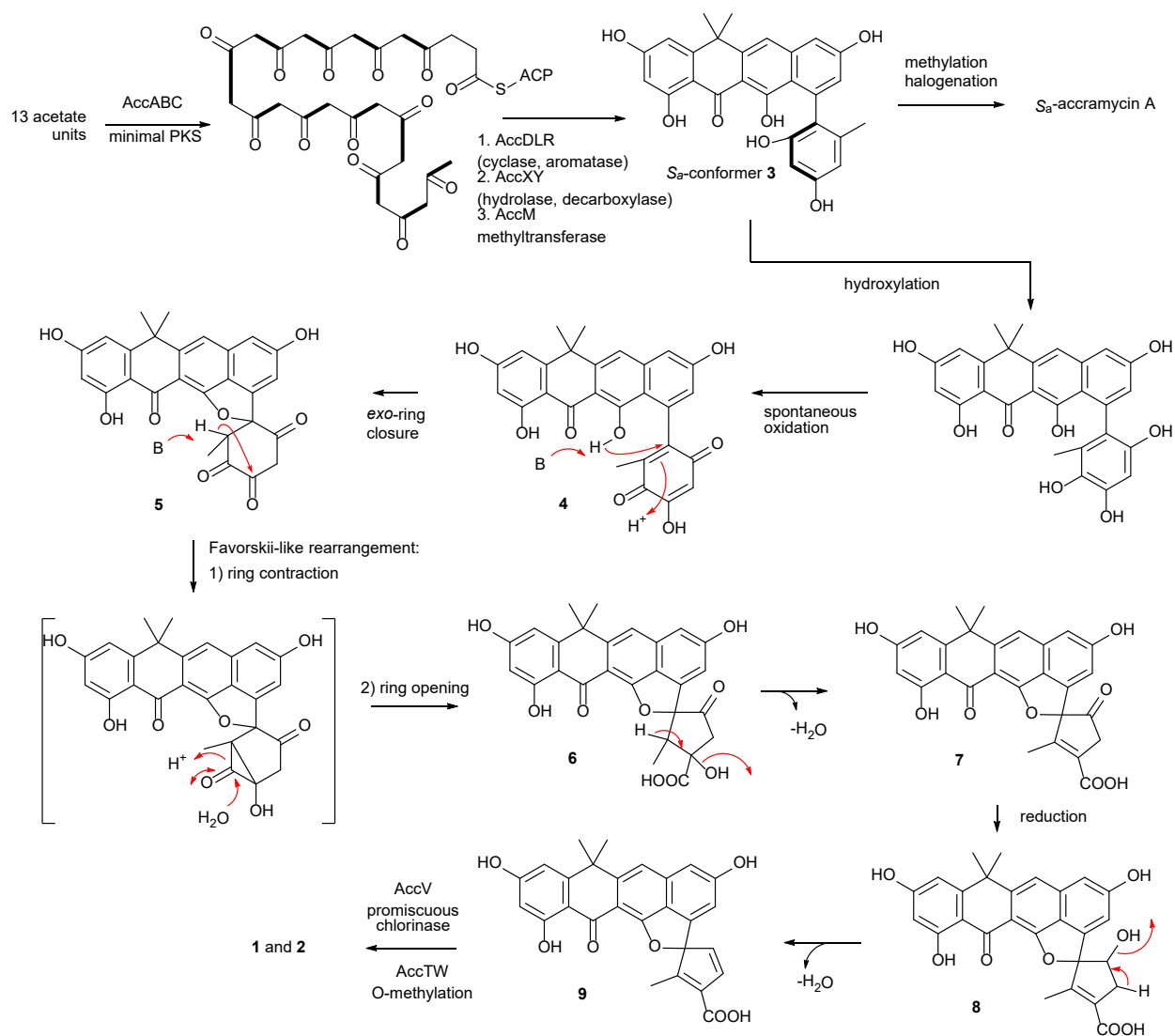
Figure 2. Experimental ECD spectra (200-400 nm) of accraspiroketide A (**1**) in methanol and the calculated ECD spectra of the model molecules of **1** at the PBE0/def2-TZVP level.

Accraspiroketides share the same [6+6+6+6] structural scaffold as polyketide-derived antibacterials, accramycin compounds (Figure S21).^{2,3} The putative enzymes encoded in the *acc* BGC are highly conserved in PNP. Hence, it is highly unlikely that the enzymes in the accramycin pathway are responsible for the unique spiro-furan structural features of **1** and **2** among PNP. However, the structural similarity between accraspiroketides and accramycins and the same carbon numbers in the backbones indicated that they should derive from a common biosynthetic intermediate **3** (Scheme 1).^{2,3} Intermediate **3** accumulated in this genetically modified $\Delta accJ$ hyper producing strain. The biosynthesis of **1** and **2** could be derailed from the original accramycin pathway to be hydroxylated by a promiscuous hydroxylase from another pathway or a housekeeping enzyme, followed by spontaneous oxidation to give the hydroxyl *ortho*-quinone **5**. The abstraction of H at the hydroxyl group at Ring C would lead to the exo-ring closure, providing **5**, which contains the 5-membered spiro furan ring system according to Baldwin's rules for ring closure. A follow-on Favorskii-type rearrangement was envisioned to provide **6** containing the last 5-membered cyclopentane ring system. Reducing the carbonyl group in **6** followed by dehydration, would give the most advanced intermediate **8**. It is likely that the promiscuous chlorination enzyme AccV and the *O*-methyltransferase AccTW would finally install the ring systems in **9** with chlorine and methoxy groups to generate **1** and **2**, respectively. AccV shows high homology (68 %/78 %) to ForV halogenase in formicamycin BGC.⁶

Favorskii-like rearrangement, although rare, has been found in bacterial polyketide metabolites.²³ The first example of naturally occurring "favorskiiases" is EncM in the biosynthesis of the antibiotic enterocin, which contains a unique tricyclic caged core.²³ EncM catalyzes the peroxyflavin-independent oxygenation-dehydrogenation dual oxidation of a highly reactive poly(β -carbonyl) thioester. More recently, the new favorskiiase, GrhO5 has been found in the

biosynthesis of the rubromycin family featuring a bisbenzannulated [5,6]-spiroketal pharmacophore.²⁴ This flavin-dependent enzyme utilizes the common intermediate, collinone, as a universal pentangular precursor to generate a [6,6]-spiroketal moiety as part of the advanced intermediate dihydrolenticulone.²⁵

However, no gene encoded for flavin-dependent favorskiiase could be identified within or in proximity to the putative *acc* BGC. A BLAST search using GrhO5 as the sequence query allowed the identification of only one open reading frame (*orf*), which encodes the protein sequence sharing high homology with GrhO5 (55 % amino acid identity). This *orf* lies in another PKS II BGC in the draft genome of MA37. The *orf* was subjected to gene inactivation to provide a double mutant. However, there was no perturbation in the production of **1** and **2** in this mutant, demonstrating no involvement of this putative flavoprotein encoding gene. The enzyme(s) responsible for the spiro system in **1** and **2** remains to be identified. It is worth noting that this is, although rare, not unprecedented as exemplified in cooperation to produce a natural product between a BGC and genes remotely located on the genome, either located or within a different BGC.²⁶⁻²⁸



Scheme 1. Proposed biosynthetic pathway for accraspiroketides A (**1**) and B (**2**)

Since aromatic polyketides often possess pharmacological properties,^{1,29} we performed antibacterial assays with **1** and **2**. Compounds **1** and **2** displayed excellent activity against *Staphylococcus aureus* (ATCC 25923), *Enterococcus faecalis* (ATCC 29212), and *Enterococcus faecium* clinical isolates (K59-68 and K60-39) with minimum inhibitory concentrations (MIC) in the range of 1.5–6.3 $\mu\text{g/mL}$ (Table 2). The addition of chlorine substituent in **2** did not enhance its bioactivity against the tested pathogens. Remarkably, **1** and **2** exhibited superior activity against *E. faecium* K60-39 than the ampicillin antibiotic (25 $\mu\text{g/mL}$) with MIC values of 4.0 $\mu\text{g/mL}$ and

4.7 $\mu\text{g/mL}$, respectively. More extensive experiments are needed to assess the modes of action of **1** and **2**. Altogether, the bioactivity profiles of **1** and **2** illustrate a promising pharmacophore for developing antibiotics that target the *E. faecium* clinical isolates.

Table 2. Minimum inhibitory concentration (MIC) values of accraspiroketide A (**1**) and accraspiroketide B (**2**)

Compound	MIC ($\mu\text{g/mL}$)			
	SA	EF	EF K59-68	EF K60-39
Accraspiroketide A (1)	3.1	3.1	1.5	4.0
Accraspiroketide B (2)	6.3	3.1	1.5	4.7
Ampicillin	0.5	1.0	1.5	25

SA - *S. aureus* (ATCC 25923), EF - *E. faecalis* (ATCC 29212), EF K59-68 - *E. faecium* K59-68, EF K60-39 - *E. faecium* K60-39

EXPERIMENTAL SECTION

General Experimental Procedures. Optical rotations were measured on an ADP 410 polarimeter (Bellingham + Stanley Ltd. 2007). NMR spectroscopic data were recorded at 25 °C on a Bruker Avance NEO 800 MHz with a He-cooled cryoprobe using methylsilane as the internal standard. The residual solvent peak was used as an internal chemical shift reference (CD_3OD : δ_{C} 49.0, δ_{H} 3.31; $\text{DMSO}-d_6$: δ_{C} 39.52, δ_{H} 2.50, CD_3CN : δ_{H} 1.3, $\delta_{\text{H}1}$ 1.93). High-resolution mass spectrometry (HRMS) analysis was performed on a Linear Trap Quadrupole (LTQ) Orbitrap coupled to an Agilent 1260 HPLC. The data were obtained in positive ion mode using the following conditions: capillary temperature 300 °C, capillary voltage 37 V, sheath gas flow rate 25 arbitrary units, auxiliary gas flow rate 20 arbitrary units, and spray voltage 4.5 kV.

Chromatographic separation was carried out using a poroshell 120 EC-C18 column (2.1 × 100 mm, 2.7 μm, Thermo Scientific, UK) with a solvent gradient from 5 % water/acetonitrile (both 0.1 % v/v formic acid) to 100 % acetonitrile (30 min, 0.5 mL/min). Semipreparative HPLC was carried out using an Agilent 1260 Infinity HPLC system with a diode array detector. Unless otherwise stated, all culture media and solvents used in the study were obtained from Fisher Scientific (UK).

Bacterial strain and culture conditions. The bacterial strain's source and the *accJ* gene deletion in *Streptomyces* sp. MA37 was previously reported.^{2,3} The $\Delta accJ$ mutant strain of MA37 was cultured in four 2-L baffled flasks containing 500 mL of ISP2 broth (4.0 g glucose, 4.0 g yeast extract, 10.0 g malt extract, in 1 L H₂O). The flasks were incubated for seven days on a rotary shaker at 180 rpm and 28 °C in the presence of light (Incu-shake FL16-2, UK).

Extraction and Isolation. At the end of 7 days, Diaion® HP-20 resin was added to the bacterial cultures (3 g/50 mL), followed by overnight incubation at the same temperature and shaking conditions (28 °C, 180 rpm). The cultures were filtered, and the resin was extracted with methanol (3×). The methanol extracts were combined and concentrated under a vacuum to yield 7.0 g of total crude extract.

The crude extract was subjected to vacuum liquid chromatography on silica gel 60 (Acros Organics™ ultra-pure 60A 40-63u) eluted with a gradient system of *n*-hexane-ethyl acetate-MeOH to give ten major fractions (F1-F10). The accraspiroketide compounds were detected in fraction 6, displaying unique UV patterns distinct from the other accramycin-containing fractions (Figures S25-S25). Fraction 6 was further fractionated with semipreparative C18 HPLC (ACE 250 × 10 mm), using a linear gradient from 95:5:0.1 (H₂O:MeOH:TFA) to 100 % MeOH for 45 minutes with a flow rate of 1.5 mL/min. The HPLC separation afforded accraspiroketides A (**1**) and B (**2**).

Accraspiroketide A (**1**). 22.2 mg; yellow solid; $[\alpha]_D^{20} -2.16$ (*c* 0.10, MeOH); UV (MeOH) λ_{\max} 180, 200, 240, 300, 400 nm; ^1H and ^{13}C NMR data, see Table 1; molecular formula: $\text{C}_{28}\text{H}_{19}\text{Cl}_3\text{O}_7$; HRESIMS m/z calculated for $\text{C}_{28}\text{H}_{20}\text{Cl}_3\text{O}_7$ $[\text{M} + \text{H}]^+ = 573.0269$; observed $[\text{M} + \text{H}]^+ = 573.0270$; $\Delta = 0.22$ ppm.

Accraspiroketide B (**2**). 0.9 mg; yellow solid; $[\alpha]_D^{20} -3.46$ (*c* 0.10, MeOH); UV (MeOH) λ_{\max} 180, 200, 240, 300, 400 nm; ^1H and ^{13}C NMR data, see Table S1; molecular formula: $\text{C}_{28}\text{H}_{18}\text{Cl}_4\text{O}_7$; HRESIMS m/z calculated for $\text{C}_{28}\text{H}_{19}\text{Cl}_4\text{O}_7$ $[\text{M} + \text{H}]^+ = 606.9879$; observed $[\text{M} + \text{H}]^+ = 606.9877$; $\Delta = -0.45$ ppm.

Calculation of theoretical ECD spectra. In general, conformational analyses were carried out via random searching in the Sybyl-X 2.0 using the MMFF94S force field with an energy cutoff of 5 kcal/mol. The results showed the four lowest energy conformers (Table S3). Subsequently, geometry optimizations and frequency analyses were implemented at the B3LYP-D3(BJ)/6-31G* level in CPCM methanol using ORCA5.0.1.³⁰ All conformers used for property calculations in this work were characterized to be stable points on potential energy surface (PES) with no imaginary frequencies. The excitation energies, oscillator strengths, and rotational strengths (velocity) of the first 60 excited states were calculated using the TD-DFT methodology at the PBE0/def2-TZVP level in CPCM methanol using ORCA5.0.1.³⁰ The ECD spectra were simulated in SpecDis V1.71 using the overlapping Gaussian function with a sigma/gamma value of 0.2 eV (half the bandwidth at 1/e peak height, sigma = 0.30 for all).³¹ Gibbs free energies for conformers were determined by using thermal correction at B3LYP-D3(BJ)/6-31G* level, and electronic energies evaluated at the wB97M-V/def2-TZVP level in CPCM methanol using ORCA5.0.1.³⁰ To get the final spectra, the simulated spectra of the conformers were averaged according to the Boltzmann distribution theory

and their relative Gibbs free energy (ΔG). By comparing the experiment spectra with the calculated model molecules, the absolute configuration of the only chiral center was determined to be *R*.

Antibacterial Assays. Compounds **1** and **2** were evaluated for antibacterial activities against *Staphylococcus aureus* ATCC 25923, *Enterococcus faecalis* ATCC 29212, and *Enterococcus faecium* clinical isolates (K59–68 and K60-39) by broth microdilution method according to published protocols.^{32–34} The clinical strains, which belonged to the complex clonal 17 sub-cluster, were obtained from the bloodstream of patients at the University Hospital of North Norway. The positive control consisted of ampicillin (Sigma), and the negative control was DMSO. The assays were performed in triplicate to determine the minimum inhibitory concentrations.

ASSOCIATED CONTENT

Supporting Information. The following files are available free of charge.

AUTHOR INFORMATION

Corresponding authors

F.M. - Department of Biology and Environmental Science, College of Science, University of the Philippines Cebu, Gorordo Ave., Lahug, Cebu City, 6000, Philippines; E-mail:

ffmaglangit@up.edu.ph

H.D. - Department of Chemistry, University of Aberdeen, Meston Walk, Aberdeen AB24 3UE, Scotland, UK; Email: h.deng@abdn.ac.uk

J.T. - School of Pharmacy and Biomedical Sciences, University of Central Lancashire, Preston, PR1 2HE, UK; Email: JTabudravu@uclan.ac.uk

A.M. - Advanced Chemistry Development (ACD/Labs) Inc., 8 King Str East, Suite 107, M5C 1B5, Toronto, Ontario, Canada; Email: arvin@acdlabs.com

Author Contributions

The manuscript was written through contributions of all authors. All authors have given approval to the final version of the manuscript.

Acknowledgements

F.M. is thankful to the Department of Science and Technology (DOST) - National Research Council of the Philippines (NRCF), DOST-Collaborative Research and Development to Leverage Philippine Economy (CRADLE) (Project no. 8647), and Department of Agriculture – Bureau of Agricultural Research. S.W. thanks Qilu Youth Scholar Startup Funding of Shangdong University. H.D. and K.K. are grateful to Leverhulme Trust-Royal Society Africa award (AA090088) and the UK Medical Research Council–UK Department for International Development (MRC/DFID) Concordat Agreement African Research Leaders Award (MR/S00520X/1). H. D. and Y. Z are grateful to the National Natural Science Foundation of China (31929001). This work was also supported by national funds from the Portuguese FCT – Fundação para a Ciência e a Tecnologia, I.P., within the projects UIDB/04564/2020 and UIDP/04564/2020. The authors thank the Laboratory for Advanced Computing (LCA) of the University of Coimbra, Portugal, for technical support. The authors would also like to acknowledge the support of the Maxwell Compute Cluster funded by the University of Aberdeen.

Notes

The authors declare no competing financial interest.

REFERENCES

- (1) Maglangit, F.; Deng, H. Cell Factory for Phenylanthracenoid Polyketide Production. *SynBio* **2023**, 1 (1), 89–102. DOI: 10.3390/synbio1010007.

(2) Maglangit, F.; Zhang, Y.; Kyeremeh, K.; Deng, H. Discovery of New Antibacterial Accramycins from a Genetic Variant of the Soil Bacterium, *Streptomyces* sp. MA37. *Biomolecules* **2020**, 10 (10), 1464. DOI: 10.3390/biom10101464.

(3) Maglangit, F.; Fang, Q.; Leman, V.; Soldatou, S.; Ebel, R.; Kyeremeh, K.; Deng, H. Accramycin A, a New Aromatic Polyketide, from the Soil Bacterium, *Streptomyces* sp. MA37. *Molecules* **2019**, 24 (18), 3384. DOI: 10.3390/molecules24183384.

(4) Feng, Z.; Chakraborty, D.; Dewell, S. B.; Reddy, B. V. B.; Brady, S. F. Environmental DNA-Encoded Antibiotics Fasamycins A and B Inhibit FabF in Type II Fatty Acid Biosynthesis. *J. Am. Chem. Soc.* **2012**, 134 (6), 2981–2987. DOI: 10.1021/ja207662w.

(5) Fukumoto, A.; Kim, Y. P.; Iwatsuki, M.; Hirose, T.; Sunazuka, T.; Hanaki, H.; Omura, S.; Shiomi, K. Naphthacemycins, Novel Circumventors of β -Lactam Resistance in MRSA, Produced by *Streptomyces* sp. KB-3346-5. II. Structure Elucidation. *J. Antibiot.* **2017**, 70 (5), 568–573. DOI: 10.1038/ja.2017.29.

(6) Qin, Z.; Munnoch, J. T.; Devine, R.; Holmes, N. A.; Seipke, R. F.; Wilkinson, K. A.; Wilkinson, B.; Hutchings, M. I. Formicamycins, Antibacterial Polyketides Produced by *Streptomyces formicae* Isolated from African Tetraponera Plant-Ants. *Chem. Sci.* **2017**, 8, 3218–3227. DOI: 10.1038/ja.2017.29.

(7) Qin, Z.; Devine, R.; Hutchings, M. I.; Wilkinson, B. Aromatic Polyketide Biosynthesis: Fidelity, Evolution and Engineering. *ChemBioChem* **2019**, 4 (7), 581074. DOI: 10.1002/cbic.200300619.

- (8) Yang, L.; Li, X.; Wu, P.; Xue, J.; Xu, L.; Li, H.; Wei, X. Streptovertimycins A–H, New Fasamycin-Type Antibiotics Produced by a Soil-Derived *Streptomyces morookaense* Strain. *J. Antibiot.* **2020**, *73* (5), 283–289. DOI: 10.1038/s41429-020-0277-6.
- (9) Li, X.; Wu, P.; Li, H.; Xue, J.; Xu, H.; Wei, X. Antibacterial and Cytotoxic Phenyltetracenoid Polyketides from *Streptomyces morookaense*. *J. Nat. Prod.* **2021**, *84* (6), 1806–1815. DOI: 10.1021/acs.jnatprod.1c00208.
- (10) Maglangit, F.; Fang, Q.; Kyeremeh, K.; Sternberg, J. M.; Ebel, R.; Deng, H. A Co-Culturing Approach Enables Discovery and Biosynthesis of a Bioactive Indole Alkaloid Metabolite. *Molecules* **2020**, *25*, 256. DOI: 10.3390/molecules25020256.
- (11) Maglangit, F.; Alrashdi, S.; Renault, J.; Trembleau, L.; Victoria, C.; Tong, M. H.; Wang, S.; Kyeremeh, K.; Deng, H. Characterization of the Promiscuous: N-Acyl CoA Transferase, LgoC, in Legonoxamine Biosynthesis. *Org. Biomol. Chem.* **2020**, *18*, 2219–2222. DOI: 10.1039/d0ob00320d.
- (12) Maglangit, F.; Tong, M. H.; Jaspars, M.; Kyeremeh, K.; Deng, H. Legonoxamines A-B, Two New Hydroxamate Siderophores from the Soil Bacterium, *Streptomyces* sp. MA37. *Tetrahedron Lett.* **2019**, *60* (1), 75–79. DOI: 10.1016/j.tetlet.2018.11.063.
- (13) Maglangit, F.; Kyeremeh, K.; Deng, H. Deletion of the Accramycin Pathway-Specific Regulatory Gene *accJ* Activates the Production of Unrelated Polyketide Metabolites. *Nat. Prod. Res.* **2022**, *37* (16), 2753–2758. DOI: 10.1080/14786419.2022.2126466.
- (14) Wu, L.; Maglangit, F.; Deng, H. Fluorine Biocatalysis. *Curr. Opin. Chem. Biol.* **2020**, *55*, 119–126. DOI: 10.1016/j.cbpa.2020.01.004.

(15) Devine, R.; McDonald, H. P.; Qin, Z.; Arnold, C. J.; Noble, K.; Chandra, G.; Wilkinson, B.; Hutchings, M. I. Re-Wiring the Regulation of the Formicamycin Biosynthetic Gene Cluster to Enable the Development of Promising Antibacterial Compounds. *Cell Chem. Biol.* **2021**, 28 (4), 515-523.e5. DOI: 10.1016/j.chembiol.2020.12.011.

(16) Elyashberg, M.; Williams, A. ACD/Structure Elucidator: 20 Years in the History of Development. *Molecules* **2021**, 26 (21), 6623. DOI: 10.3390/molecules26216623.

(17) Elyashberg, M.; Blinov, K.; Molodtsov, S.; Williams, A. J. Structure Revision of Asperjinone Using Computer-Assisted Structure Elucidation Methods. *J. Nat. Prod.* **2013**, 76 (1), 113–116. DOI: 10.1021/np300218g.

(18) Kutateladze, A. G.; Bates, R. W.; Elyashberg, M.; Williams, C. M. Structural Reassignment of Two Polyenol Natural Products. *European J. Org. Chem.* **2023**, 26 (9). DOI: 10.1002/ejoc.202201316.

(19) Elyashberg, M.; Novitskiy, I. M.; Bates, R. W.; Kutateladze, A. G.; Williams, C. M. Reassignment of Improbable Natural Products Identified through Chemical Principle Screening. *European J. Org. Chem.* **2022**, 2022 (34). DOI: 10.1002/ejoc.202200572.

(20) Elyashberg, M. E.; Williams, A.; Blinov, K. Contemporary Computer-Assisted DOI: 10.1039/9781849734578.

(21) Elyashberg, M. E.; Blinov, K. A.; Williams, A. J.; Molodtsov, S. G.; Martin, G. E.; Martirosian, E. R. Structure Elucidator: A Versatile Expert System for Molecular Structure Elucidation from 1D and 2D NMR Data and Molecular Fragments. *J. Chem. Inf. Comput. Sci.* **2004**, 44 (3), 771–792. DOI: 10.1021/ci0341060.

(22) Pretsch, E.; Bühlmann, P.; Affolter, C. Structure Determination of Organic Compounds, 3rd ed.; *Springer Berlin, Heidelberg*, **2000**. DOI: 10.1007/978-3-662-04201-4.

(23) Teufel, R.; Miyanaga, A.; Michaudel, Q.; Stull, F.; Louie, G.; Noel, J. P.; Baran, P. S.; Palfey, B.; Moore, B. S. Flavin-Mediated Dual Oxidation Controls an Enzymatic Favorskii-Type Rearrangement. *Nature* **2013**, 503 (7477), 552–556. DOI: 10.1038/nature12643.

(24) Toplak, M.; Saleem-Batcha, R.; Piel, J.; Teufel, R. Catalytic Control of Spiroketal Formation in Rubromycin Polyketide Biosynthesis. *Angew. Chemie - Int. Ed.* **2021**, 60 (52), 26960–26970. DOI: 10.1002/anie.202109384.

(25) Frensch, B.; Lechtenberg, T.; Kather, M.; Yunt, Z.; Betschart, M.; Kammerer, B.; Lüdeke, S.; Müller, M.; Piel, J.; Teufel, R. Enzymatic Spiroketal Formation via Oxidative Rearrangement of Pentangular Polyketides. *Nat. Commun.* **2021**, 12 (1), 4–15. DOI: 10.1038/s41467-021-21432-9.

(26) Shen, Y.; Sun, F.; Zhang, L.; Cheng, Y.; Zhu, H.; Wang, S. P.; Jiao, W. H.; Leadlay, P. F.; Zhou, Y.; Lin, H. W. Biosynthesis of Depsipeptides with a 3-Hydroxybenzoate Moiety and Selective Anticancer Activities Involves a Chorismatase. *J. Biol. Chem.* **2020**, 295 (16), 5509–5518. DOI: 10.1074/jbc.RA119.010922.

(27) Li, S.; Guo, J.; Reva, A.; Huang, F.; Xiong, B.; Liu, Y.; Deng, Z.; Leadlay, P. F.; Sun, Y. Methyltransferases of Gentamicin Biosynthesis. *Proc. Natl. Acad. Sci. U.S.A.* **2018**, 115 (6), 1340–1345. DOI: 10.1073/pnas.1711603115.

(28) Lazos, O.; Tosin, M.; Slusarczyk, A. L.; Boakes, S.; Cortés, J.; Sidebottom, P. J.; Leadlay, P. F. Biosynthesis of the Putative Siderophore Erythrochelin Requires Unprecedented Crosstalk

between Separate Nonribosomal Peptide Gene Clusters. *Chem. Biol.* **2010**, 17 (2), 160–173. DOI: 10.1016/j.chembiol.2010.01.011.

(29) Hertweck, C. The Biosynthetic Logic of Polyketide Diversity. *Angew. Chemie - Int. Ed.* **2009**, 48 (26), 4688–4716. DOI: 10.1002/anie.200806121.

(30) Neese, F.; Wennmohs, F.; Becker, U.; Riplinger, C. The ORCA Quantum Chemistry Program Package. *J. Chem. Phys.* **2020**, 152 (22). DOI: 10.1063/5.0004608.

(31) Philip J. Stephens; Nobuyuki Harada. ECD Cotton Effect Approximated by the Gaussian Curve and Other Methods. *Chirality* **2010**, 22, 229–233. DOI: 10.1002/chir.

(32) Fang, Q.; Maglangit, F.; Mugat, M.; Urwald, C.; Kyeremeh, K.; Deng, H. Targeted Isolation of Indole Alkaloids from *Streptomyces* sp. CT37. *Molecules* **2020**, 25 (1108).

(33) Fang, Q.; Maglangit, F.; Wu, L.; Ebel, R.; Kyeremeh, K.; Andersen, J. H.; Annang, F.; Pérez-Moreno, G.; Reyes, F.; Deng, H. Signalling and Bioactive Metabolites from *Streptomyces* sp. RK44. *Molecules* **2020**, 25, 460. DOI: 10.3390/molecules25030460.

(34) Cockerill, F. I.; Wikler, M. A.; Alder, J.; Dudley, M. N.; Eliopoulos, G. M.; Ferraro, M. J.; Hardy, D. J.; Hecht, D. W.; Hindler, J. A.; Patel, J. B.; Powell, M.; Swenson, J. M.; Richard B. Thomson, J.; Traczewski, M. M.; Turnidge, J. D.; Weinstein, M. P.; Zimmer, B. L. MO7-A9 Methods for Dilution Antimicrobial Susceptibility Tests for Bacteria That Grow Aerobically; Approved Standard — Ninth Edition. *Clin. Lab. Stand. Inst.* **2012**, 32 (2), 1–67. DOI: 10.4103/0976-237X.91790.